Since January 2020 Elsevier has created a COVID-19 resource centre with free information in English and Mandarin on the novel coronavirus COVID-19. The COVID-19 resource centre is hosted on Elsevier Connect, the company's public news and information website.

Microbial Pathogenesis 149 (2020) 104546

Contents lists available at ScienceDirect

Microbial Pathogenesis

journal homepage: www.elsevier.com/locate/micpath

Novel cyclohexanone compound as a potential ligand against SARS-CoV-2 main-protease

Soumya Basu [a], Balaji Veeraraghavan [b], Sudha Ramaiah [a], Anand Anbarasu [a,*]

[a] Medical & Biological Computing Laboratory, School of Bio-sciences & Technology, Vellore Institute of Technology, Vellore, 632014, Tamil Nadu, India
[b] Department of Clinical Microbiology, Christian Medical College & Hospital, Vellore, 632004, Tamil Nadu, India

ARTICLE INFO

Keywords:
SARS-CoV-2 mpro
Docking
Molecular dynamics simulation
Anti-viral activity
Pharmacokinetics

ABSTRACT

No commercially available drug candidate has yet been devised which is unique to and not repurposed against SARS-CoV-2 and has high efficacy or safe toxicity profile or both. Taking curcumin as a reference compound, we identified a new commercially available cyclohexanone compound, ZINC07333416 with binding energy (−8.72 kcal/mol) better than that of popularly devised *anti*-Covid-19 drugs like viral protease inhibitor Lopinavir, nucleoside analogue Remdesivir and the repurposed drug hydroxychloroquine when targeted to the active-site of SARS-CoV-2 Main protease (Mpro) through docking studies. The ligand ZINC07333416 exhibits crucial interactions with major active site residues of SARS-CoV-2 Mpro viz. Cys145 and His41 involving in the protease activity; as well as GLU-166 and ASN-142 which plays the pivotal role in the protein-dimerization. The protein-ligand stable interaction was further confirmed with molecular dynamics simulation (MDS) studies. Based on virtual assessment, ZINC07333416 also have significant values in terms of medicinal chemistry, pharmacokinetics, synthetic accessibility and anti-viral activity that encourage its experimental applications against COVID-19.

The novel coronavirus SARS-CoV-2, etiological agent of COVID-19 have engendered a pandemic with higher morbidity and mortality rates. Millions of registered victims and several hundred thousand deaths have been reported worldwide due to COVID-19 [1]. Although many compounds have been advised and tested against COVID-19, most of them were either repurposed drugs or they lacked efficacy or lacked safe toxicity profile or all of them [2,3]. Drug repurposing against a pandemic may result in sudden crisis of an essential drug; it may also not provide a long term efficacy or may result in unfavourable off-site interactions [3]. In our present study, we have focused on the identification of a novel compound targeted to SARS-CoV-2 main protease (Mpro) since, protease inhibitor drugs have shown improved outcome in COVID-19 victims [3]. We also objectified on comparing the same with popular drugs devised against COVID-19 [3–5] in terms of interaction, toxicity profiles and drug properties *in-silico*.

Curcumin was chosen in our study as a reference to screen analogous compounds since it has anti-viral activity and a safe toxicity profile [6,7]. The three-dimensional (3D) structure of SARS-COV-2 Mpro (6LU7) was retrieved from RCSB-protein databank and all ligands (drugs/compounds) were obtained from PubChem database. The 3D formatting of ligands was performed using Openbabel tool [8]. 400 commercially available curcumin analogues were identified through SwissSimilarity server based on their stereochemistry, structural alignment and pharmacophore model [9]. Screened compounds (similarity scores with curcumin > 0.7) and known reference compounds were docked onto SARS-COV-2 Mpro using AutoDock version 4.2 [10]. Prior to the docking analysis, structure of the target protein was optimized by removing crystallographic water molecules and unwanted hetero-atoms or other bound ligands. Polar hydrogens were added and non-polar hydrogens were merged thereafter to the protein in ideal geometry. Requisite Kollman charges (4.0) were added to the protein to finally stabilize its structure. The torsions were fixed for the ligands. The initial parameters and van der Waals well depth of 0.100 kcal/mol was assigned for the protein. The important active site residue His41 [11] was centred to construct affinity grid-box of 60 $Å^3$. Lamarckian Genetic Algorithm was employed to generate SARS-COV-2 Mpro-ligand complexes in 10 different poses. Based on best poses and lowest of binding energies we identified the phenolic compound ZINC07333416 having a 2, 6 di-methylene-cyclohexanone group Fig. 1a. The binding energy of our lead compound ZINC07333416 (−8.72 kcal/mol) is

* Corresponding author.
E-mail addresses: soumya.basu@vit.ac.in (S. Basu), vbalaji@cmcvellore.ac.in (B. Veeraraghavan), sudhaanand@vit.ac.in (S. Ramaiah), aanand@vit.ac.in (A. Anbarasu).

https://doi.org/10.1016/j.micpath.2020.104546
Received 28 April 2020; Received in revised form 6 July 2020; Accepted 28 September 2020
Available online 1 October 2020

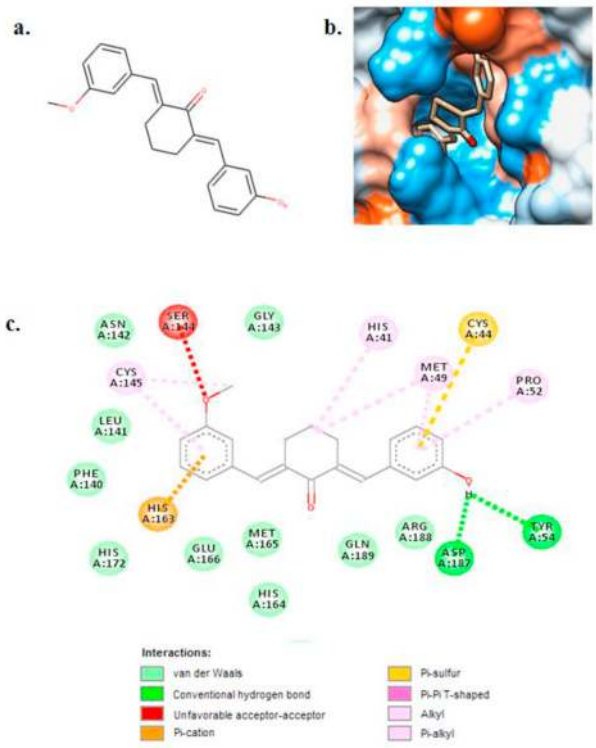

Fig. 1. Interaction of lead compound with SARS-CoV-2 Mpro. a. The chemical structure of our lead compound ZINC07333416. b. Lead bound within the active site binding pocket of SARS-COV-2 Mpro. c. ZINC07333416 exhibiting interaction with crucial active-site residues responsible for structural and functional integrity of the protease.

better than that of our reference compound Curcumin (−6.9 kcal/mol), tested viral protease inhibitor Lopinavir [2] (−8.29 kcal/mol), newly identified Lopinavir analogue ZINC541677852 [3] (−7.72 kcal/mol), popular anti-viral nucleoside analogue Remdesivir [5] (−6.18 kcal/-mol) and the repurposed drug hydroxychloroquine [4] (−6.36 kcal/-mol) when targeted to the active-site of SARS-COV-2 Mpro (Table 1).

Fig. 1 c. shows the ligand ZINC07333416 exhibiting Pi-alkyl interactions with both of the crucial active site residues Cys145 and His41 that plays the major role in the protease activity [11]. Conventional hydrogen bond was found with active site residues ASP-187 and TYR-54. The ligand also exhibits van der Waals interaction with GLU-166 and ASN-142 which plays the pivotal role in dimerization [11] of the protein. Hence, ZINC07333416 can efficiently bind to the active site of the SARS-COV-2 Mpro by specifically interacting with residues responsible for structural and functional integrity of the protease.

AVCpred server was employed to predict the general antiviral potential of our lead as well as reference compounds (see Table 2). The prediction uses integrated Quantitative-Structure-Activity-Relationship (QSAR) and best-performing molecular descriptor based screening-algorithm against 30 known viral pathogens including SARS coronavirus, Human Immunodeficiency Virus (HIV), Respiratory Syncytial Virus etc. [12] The general anti-viral activity of ZINC07333416 was found to be 41.95%, which is not only higher than that of hydroxychloroquine (37.74%) and curcumin (20.18%) but also higher than other commercially available curcumin analogues (similarity score > 0.7) (Supplementary file). The drug-likeliness, pharmacokinetics and medicinal chemistry of ZINC07333416 predicted by *SwissADME* server [13] shows significantly low values of logP (3.11), polar surface area (46.53) and synthetic accessibility (2.83) (Table 2). These values depict the favourable bioavailability, cellular permeability, renal clearance and ease to make properties of ZINC07333416 respectively [14,15]. High capabilities of gastrointestinal absorption (signifying oral administration possibilities) and blood-brain barrier permeation of ZINC07333416 were also predicted as compared to popular anti-viral drugs (Supplementary file).

ProtoxII server [16] showed a higher LD_{50} value of ZINC07333416 (2300 mg/kg) designating its fairly non-toxic nature as compared to ZINC541677852 (1000 mg/kg) and hydroxychloroquine (1240 mg/kg) (Table 2). No carcinogenicity and/or mutagenicity were predicted by ProtoxII for ZINC07333416 as compared to hydroxychloroquine or other tested anti-viral compounds (not shown).

Molecular dynamics simulation (MDS) study was employed to assess the interaction-dynamics of protein-ligand complex at an atomic level as a function of time. GROMACS 5.0.2 package with GROMOS9643a1 force-field was used. Ligand topology was built with ProDRG 2.5 server. The protein-ligand complex was placed in the centre of a cubic box with a uniform edge-distance of 1.2 nm. The sample was solvated with simple-point-charge water model followed by neutralizing the system by adding requisite counter ions (Na or Cl). Energy minimization was thereafter performed with 50,000 steps and 1000 kJ/mol nm^{-1} convergence-tolerance using steepest descent algorithm. The system was equilibrated with standard NVT (constant number of particles, volume and temperature) and NPT (constant number of particles, pressure and temperature) ensembles for 150 ps Particle-Mesh Ewald electrostatics (PME) summation was used for treating long-range electrostatic interactions with an order of 4.0 and Fourier spacing of 0.16 nm. Finally, production MD was performed for 50 ns timescale.

From the root mean square deviation (RMSD) graphs, it was observed that for target protein Fig. 2 (A) the trajectory attained equilibrium beyond 10ns with a mean value around 0.25 nm. RMSD of ligand ZINC07333416 Fig. 2 (B) was almost stable throughout the course of simulation with a mean value around 0.25 nm. The similar mean values are an indicative of minimum relative variation of ligand position than that of the protein, thereby ascertaining the stability of ligand-protein binding pose.

The low average value (2.05 nm) and stable trajectory of Radius of gyration (Rg) Fig. 2 (C) ensured the compactness of the protein-ligand complex during MDS. Similarly, a stable solvent accessible surface area (SASA) of 135–140 nm^2 Fig. 2 (D) revealed the compactness of the hydrophobic core and hence the stable conformational geometry of the protein-ligand complex during MDS. Although our target protein and ligand tried to interact with three to five hydrogen bonds during the course of simulation, only two hydrogen bonds were found to be consistent throughout the simulation Fig. 2 (E) which is perfectly in sync

Table 1
Binding energies of our lead compound ZINC07333416 as compared to other studied compounds.

Protein	Ligands		Binding energy (kcal/mol)
SARS CoV2 (2019-nCoV) Mpro	Lead compound	ZINC07333416	−8.72
	(Commercially available Curcumin analogue)		
	Newly addressed compounds	Hydroxychloroquine	−6.36
		ZINC541677852	−7.72
	Curcumin		−6.90
	(reference compound)		
	Popular antiviral drugs devised	Remdesivir (nucleoside analogue)	−6.18
		Lopinavir (viral protease inhibitor)	−8.29

Table 2
Important medicinal, toxicity and antiviral properties of studied compounds (TPSA = total polar surface area; GI = gastro-intestinal; BBB = blood brain barrier).

Compounds	Molecular weight	mlogP	TPSA	Drug likeliness violations	Lead likeliness violations	GI absorption	BBB permeation	Synthetic access-ibility Score [Scale: 1 (very easy) to 10 (difficult)]	LD50 (mg/kg)	Anti-viral activity (%)
ZINC07333416	320.38	3.11	46.53	No	1	High	Yes	2.83	2300	41.95
Hydroxy-chloroquine	335.87	2.35	48.39	No	2	High	Yes	2.82	1240	37.74
ZINC541677852	394.39	2.92	76.02	No	1	High	Yes	3.60	1000	72.54
Curcumin	368.38	1.47	93.07	No	2	High	No	2.97	2000	20.18
Remdesivir	602.59	2.82	203.57	Yes	2	Low	No	6.33	1000	Proven
Lopinavir	628.80	2.93	120.00	Yes	3	High	No	5.67	5000	Proven

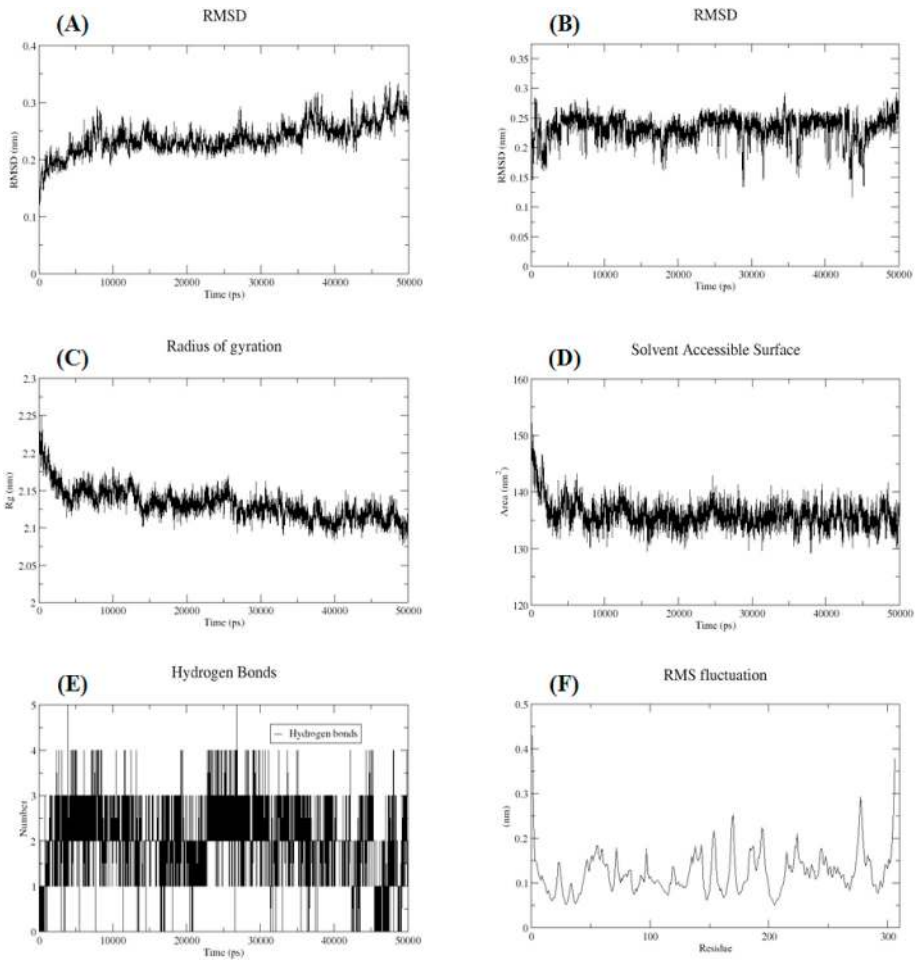

Fig. 2. (A) RMSD trajectory of SARS CoV-2 Mpro. (B) RMSD trajectory of ligand ZINC07333416. (C) Rg pattern of the protein-ligand complex during MDS. (D) SASA to evaluate stability of hydrophobic core of the complex backbone. (E) H-bond observed during MDS. (F) RMSF pattern of target protein during simulation.

with our docking results. The root mean square fluctuation (RMSF) was used to evaluate the amount of positional fluctuation of each residue of the protein-ligand backbone during MDS. It was observed that our RMSF values lie between 0.05 and 0.4 nm with an approximate average of 0.2 nm and minimum fluctuations of the crucial active-site residues Fig. 2 (F). The DSSP (Define Secondary Structure of Proteins) model further ensured the stability of the protein structure during simulation by ascertaining the changes in secondary structures. The study revealed that stable secondary structural conformation of our target protein with bound ligand was maintained throughout the simulation with respect to all structural patterns (helices, loops, bends etc.) Fig. 3.[17–19].

Therefore, we identified a new and commercially available compound having favourable drug-likeliness, lead-likeliness and synthetic accessibility. The identified compound showed stable molecular interactions when targeted to the active-site of SARS CoV-2 Mpro. It has no experimental or clinical report so far and hence can be uniquely addressed to COVID-19 to overcome the drawbacks with repurposed drugs. Furthermore, the anti-viral activity, medicinal chemistry and toxicity profiles of our lead compound are encouraging as compared to known/tested compounds and hence can be optimistically used for experimental trials against COVID-19.

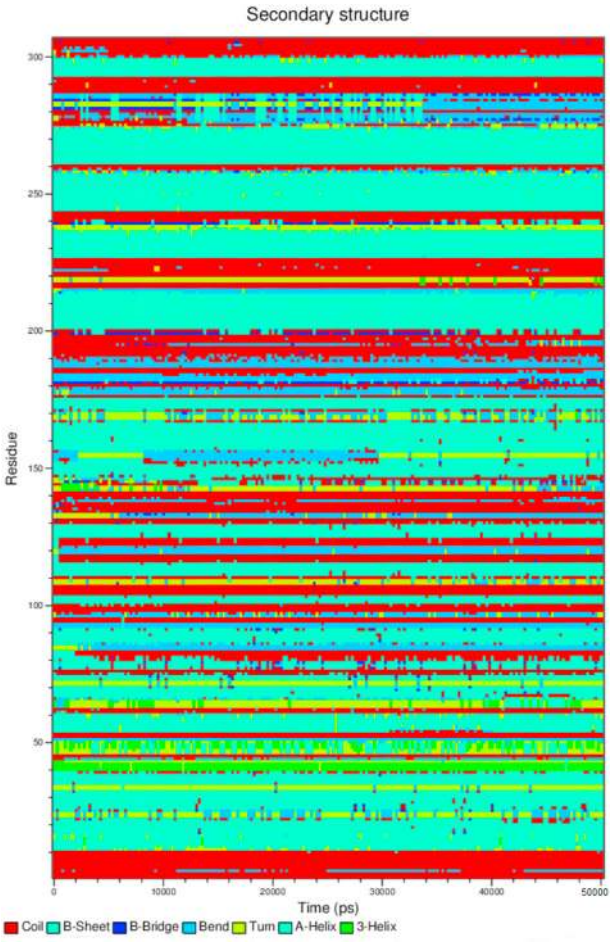

Fig. 3. Structural analysis by DSSP algorithm showing stable secondary structural conformation during 50 ns timescale.

Declaration of competing interest

The authors declare that there is no conflict of interest.

Acknowledgement

The authors would like to thank the management of Vellore Institute of Technology for providing the necessary facilities to carry out this research. The authors would also like to thank Mr. Miryala Sravan Kumar for his help in carrying out the molecular dynamic simulations.

Appendix A. Supplementary data

Supplementary data to this article can be found online at https://doi.org/10.1016/j.micpath.2020.104546.

Funding

Indian Council of Medical Research (ICMR), Govt. of India, Adhoc research grant IRIS-ID:2019-0810.

References

[1] Coronavirus Disease 2019-Situation Report-97, World Heal. Organ., 2020, p. 2633, https://doi.org/10.1001/jama.2020.2633.

[2] B. Cao, Y. Wang, D. Wen, W. Liu, J. Wang, G. Fan, L. Ruan, B. Song, Y. Cai, M. Wei, X. Li, J. Xia, N. Chen, J. Xiang, T. Yu, T. Bai, X. Xie, L. Zhang, C. Li, Y. Yuan, H. Chen, H. Li, H. Huang, S. Tu, F. Gong, Y. Liu, Y. Wei, C. Dong, F. Zhou, X. Gu, J. Xu, Z. Liu, Y. Zhang, H. Li, L. Shang, K. Wang, K. Li, X. Zhou, X. Dong, Z. Qu, S. Lu, X. Hu, S. Ruan, S. Luo, J. Wu, L. Peng, F. Cheng, L. Pan, J. Zou, C. Jia, J. Wang, X. Liu, S. Wang, X. Wu, Q. Ge, J. He, H. Zhan, F. Qiu, L. Guo, C. Huang, T. Jaki, F.G. Hayden, P.W. Horby, D. Zhang, C. Wang, A trial of lopinavir-ritonavir in adults hospitalized with severe covid-19, N. Engl. J. Med. (2020) 1–13, https://doi.org/10.1056/NEJMoa2001282.

[3] A.T. Ton, F. Gentile, M. Hsing, F. Ban, A. Cherkasov, Rapid identification of potential inhibitors of SARS-CoV-2 main protease by deep docking of 1.3 billion compounds, Mol. Inform. 39 (2020) 1–8, https://doi.org/10.1002/minf.202000028.

[4] J. Liu, R. Cao, M. Xu, X. Wang, H. Zhang, H. Hu, Y. Li, Z. Hu, W. Zhong, M. Wang, Hydroxychloroquine, a less toxic derivative of chloroquine, is effective in inhibiting SARS-CoV-2 infection in vitro, Cell Discov 6 (2020) 16, https://doi.org/10.1038/s41421-020-0156-0.

[5] M. Wang, R. Cao, L. Zhang, X. Yang, J. Liu, M. Xu, Z. Shi, Z. Hu, W. Zhong, G. Xiao, Remdesivir and chloroquine effectively inhibit the recently emerged novel coronavirus (2019-nCoV) *in vitro*, Cell Res. 30 (2020) 269–271, https://doi.org/10.1038/s41422-020-0282-0.

[6] D. Kumar, S. Basu, L. Parija, D. Rout, S. Manna, J. Dandapat, P.R. Debata, Curcumin and Ellagic acid synergistically induce ROS generation, DNA damage, p53 accumulation and apoptosis in HeLa cervical carcinoma cells, Biomed. Pharmacother. 81 (2016) 31–37, https://doi.org/10.1016/j.biopha.2016.03.037.

[7] D. Ting, N. Dong, L. Fang, J. Lu, J. Bi, S. Xiao, H. Han, Multisite inhibitors for enteric coronavirus: antiviral cationic carbon dots based on curcumin, ACS Appl. Nano Mater. 1 (2018) 5451–5459, https://doi.org/10.1021/acsanm.8b00779.

[8] N.M. O'Boyle, M. Banck, C.A. James, C. Morley, T. Vandermeersch, G. R. Hutchison, Open babel: an open chemical toolbox, J. Cheminf. 3 (2011) 33, https://doi.org/10.1186/1758-2946-3-33.

[9] V. Zoete, A. Daina, C. Bovigny, O. Michielin, Swiss similarity: a web tool for low to ultra high throughput ligand-based virtual screening, J. Chem. Inf. Model. 56 (2016) 1399–1404, https://doi.org/10.1021/acs.jcim.6b00174.

[10] G.M. Morris, W. Huey R Fau - Lindstrom, M.F. Lindstrom W Fau - Sanner, R. K. Sanner Mf Fau - Belew, D.S. Belew Rk Fau - Goodsell, A.J. Goodsell Ds Fau - Olson, A.J. Olson, J.C. Chem, Autodock 4 and autodocktools 4: automated docking with selective receptor flexibility, J. Comput. Chem. 30 (2009) 2785–2791, https://doi.org/10.1002/jcc.21256.

[11] A. Paasche, A. Zipper, S. Schäfer, J. Ziebuhr, T. Schirmeister, B. Engels, Evidence for substrate binding-induced zwitterion formation in the catalytic cys-his dyad of the SARS-CoV main protease, Biochemistry 53 (2014) 5930–5946, https://doi.org/10.1021/bi400604t.

[12] A. Qureshi, G. Kaur, M. Kumar, AVCpred: an integrated web server for prediction and design of antiviral compounds, Chem. Biol. Drug Des. 89 (2017) 74–83, https://doi.org/10.1111/cbdd.12834.

[13] A. Daina, O. Michielin, V. Zoete, SwissADME: a free web tool to evaluate pharmacokinetics, drug-likeness and medicinal chemistry friendliness of small molecules, Sci. Rep. 7 (2017) 42717, https://doi.org/10.1038/srep42717.

[14] K.M. Honorio, T.L. Moda, A.D. Andricopulo, Pharmacokinetic properties and in silico ADME modeling in drug discovery, Med. Chem. 9 (2013) 163–176, https://doi.org/10.2174/1573406411309020002.

[15] P. Ertl, A. Schuffenhauer, Estimation of synthetic accessibility score of drug-like molecules based on molecular complexity and fragment contributions, J. Cheminf. 1 (2009) 8, https://doi.org/10.1186/1758-2946-1-8.

[16] P. Banerjee, A.O. Eckert, A.K. Schrey, R. Preissner, ProTox-II: a webserver for the prediction of toxicity of chemicals, Nucleic Acids Res. 46 (2018) 257–263, https://doi.org/10.1093/nar/gky318.

[17] M. Jayaraman, S.K. Rajendra, K. Ramadas, Structural insight into conformational dynamics of non-active site mutations in KasA: a Mycobacterium tuberculosis target protein, Gene 720 (2019) 144082, https://doi.org/10.1016/j.gene.2019.144082.

[18] K. Muthu, M. Panneerselvam, N.S. Topno, M. Jayaraman, K. Ramadas, Structural perspective of ARHI mediated inhibition of STAT3 signaling: an insight into the inactive to active transition of ARHI and its interaction with STAT3 and importinβ, Cell. Signal. 27 (2015) 739–755, https://doi.org/10.1016/j.cellsig.2014.11.036.

[19] M. Thillainayagam, S. Ramaiah, A. Anbarasu, Molecular docking and dynamics studies on novel benzene sulfonamide substituted pyrazole-pyrazoline analogues as potent inhibitors of plasmodium falciparum histo aspartic protease, J. Biomol. Struct. Dyn. (2019) 1–11, https://doi.org/10.1080/07391102.2019.1654923, 0.